Department of Veterans Affairs

Journal of Rehabilitation Research and Development Vol. 37 No. 2, March/April 2000
Pages 135–143

Mechanobiology of tendon adaptation to compressive loading through fibrocartilaginous metaplasia

Tishya A.L. Wren, PhD; Gary S. Beaupré, PhD; Dennis R. Carter, PhD
Rehabilitation Research & Development Center, Veterans Affairs Health Care System, Palo Alto, CA 94304; Biomechanical Engineering Division, Mechanical Engineering Department, Stanford University, Stanford, CA 94305

Abstract—Tendons that wrap around bones often undergo fibrocartilaginous metaplasia. In this paper, we examine the biomechanical causes and consequences of this metaplasia. We propose an adaptation rule in which tissue permeability changes in response to local cyclic hydrostatic pressures associated with physical activity. The proposed rule predicts the development of a low-permeability region corresponding to the fibrocartilaginous region in a representative wrap-around tendon. A poroelastic finite element model is used to examine the time-dependent fluid pressures and compressive stresses and strains in the solid constituents of the tendon's extrafibrillar matrix. The low permeability in the adapted fibrocartilaginous region maintains fluid pressures, protecting the solid constituents of the tendon's extracellular matrix from high compressive stresses and strains that could disrupt the matrix organization. Adaptation through fibrocartilaginous metaplasia therefore allows wrap-around tendons to function effectively over a lifetime without sustaining excessive mechanical damage due to cyclic compressive loading.

Key words: *adaptation, damage, fibrocartilage, tendon.*

This material is based upon work supported by the Veterans Administration Rehabilitation Research and Development Program, Washington, DC 20420.

Address all correspondence and requests for reprints to: Tishya A.L. Wren, PhD, VA Palo Alto RR&D Center (153), 3801 Miranda Avenue, Palo Alto, CA 94304; email: wren@stanford.edu.

INTRODUCTION

Tendons normally consist of dense fibrous tissue in which type I collagen fibers are aligned along the tendon's long axis. While this structure allows tendons to withstand the high tensile loads imposed on them during normal activities of daily living, it is poorly suited to withstanding compressive loading, and many tendons are subjected to localized compressive loading in regions where they wrap around bony pulleys or pass beneath fibrous retinacula (1). Tendons often undergo fibrocartilaginous metaplasia in these regions. Benjamin et al. (2) identified fibrocartilage in 22 of 38 wrap-around tendon sites from the human body they examined. Currently, the relationships between tendon mechanics and fibrocartilaginous metaplasia are not well understood. This paper provides a framework to better understand the biomechanical causes and consequences of fibrocartilaginous metaplasia in tendons.

Tendon fibrocartilage differs substantially from normal tendinous tissue, containing 76 percent water by wet weight, compared with 54–57 percent for normal tendinous tissue (3). The fibrocartilage has a proteoglycan content five times higher than other regions of the tendon (3), and its glycosaminoglycan content is 2–10 times that of normal tendinous tissue (4,5).

Northern blot analysis has shown that mRNA for aggrecan, type II collagen, biglycan, and decorin is highly expressed in cells from the fibrocartilaginous region of adult tendon but only mRNA for decorin is highly expressed in cells from the tendinous region (6). In addition, fibrocartilage contains rounded cells, arranged in columns and often located in lacunae, instead of the elongated fibroblasts found in normal tendinous tissue (3). These differences all indicate that cells in the fibrocartilaginous region have taken on a chondrocytic phenotype, while cells in the rest of the tendon have not. The changes in cell phenotype and biosynthetic activity likely result from differences in their local mechanical environments.

In vitro studies have correlated the biosynthetic activity of connective tissue cells with the mechanical loading imposed on them. Fibroblasts, normally elongated *in vivo*, produce fibrous matrix constituents, including type I collagen, when exposed to cyclic tensile strains (7). When fibroblasts become rounded, however, they decrease their production of fibrous matrix constituents and secrete enzymes that degrade the fibrous matrix (8,9). Chondrocytes, on the other hand, normally assume a round shape and produce cartilaginous matrix constituents when in this shape. Static hydrostatic pressures (compressive stresses of equal magnitude from all directions) between 2.6 and 15 MPa increase the incorporation of radiolabeled markers in cartilage explants, indicating up-regulation of proteoglycan, protein, and RNA synthesis (10,11). Static and dynamic hydrostatic compression of cultured chondrocytes also elevate glycosaminoglycan synthesis and mRNA levels for aggrecan and type II collagen (12). In contrast, cyclic tensile loading stimulates collagen synthesis by chondrocytes without increasing proteoglycan synthesis (13).

A tissue differentiation theory consistent with these *in vitro* observations was proposed by Pauwels (14) and further developed by Carter and colleagues (15,16), who hypothesized that compressive hydrostatic stresses stimulate the production of cartilaginous matrix constituents while distortional or tensile strains stimulate the production of fibrous matrix constituents. Giori et al. (17) applied this hypothesis to wrap-around tendons using an elastic finite element model of the rabbit flexor digitorum profundus tendon. They found that the entire tendon experiences significant distortional strains that would maintain the fibrous tissue phenotype. The region adjacent to the bone also experiences significant compressive hydrostatic stresses that would stimulate production of cartilaginous matrix constituents. This region should therefore exhibit a fibrocartilaginous phenotype, as indeed it does.

The current study builds on the work of Giori et al. (17) in examining compressive hydrostatic stresses as a stimulus for fibrocartilaginous metaplasia in tendons. In addition, the current study considers the biomechanical consequences of the metaplasia. As described above, the metaplasia results in increased aggrecan content in the fibrocartilaginous region. As in articular cartilage, the aggrecan restricts fluid flow, leading to reduced tissue permeability in the fibrocartilaginous region (18,19). To study the effects of this reduced permeability, we employ a poroelastic model of the rabbit flexor digitorum profundus tendon. Poroelastic and biphasic models are often used to represent cartilaginous and fibrocartilaginous tissues (18,20–22). Poroelastic and biphasic models are equivalent when the fluid phase is inviscid, as is usually assumed (23,24). The poroelastic model treats the tissue as a porous solid structure saturated with water that flows through the tissue in response to pressure gradients. Fluid flow is governed by tissue permeability, in that flow through a tissue with high permeability is more rapid than flow through a tissue with low permeability. Stresses in the tissue are shared between the fluid and solid phases, with the distribution between phases changing over time.

In the following sections, we first examine the general behavior of the poroelastic model using a tendon with homogeneous high permeability. We then compare the behavior of this tendon with that of a tendon having homogeneous low permeability. Finally, we consider an adaptation simulation in which a tendon of homogeneous high permeability undergoes permeability reductions in regions experiencing high cyclic hydrostatic pressures during physiologic loading. This adaptation simulates chondroid metaplasia in the tendon where it pushes against the bone. Both fluid pressures and total hydrostatic pressures (sum of fluid pressures and compressive hydrostatic stresses in the solid phase) are considered as mechanical stimuli for the adaptation. We compare the results using these stimuli with the results from the single-phase elastic model (17). The results provide insight into the mechanisms that enable tendons to function effectively for an entire lifetime despite their exposure to different mechanical environments.

METHODS

This study used a finite element model similar to that proposed by Giori and colleagues (17). Both models were implemented using the ABAQUS finite element code (Hibbit, Karlsson and Sorensen, Inc., Providence, RI). The two models have an identical geometry reflecting the anatomy of the rabbit flexor digitorum profundus tendon wrapping around the talus. **Figure 1** shows the finite element mesh, boundary conditions, and applied loading used in this study.

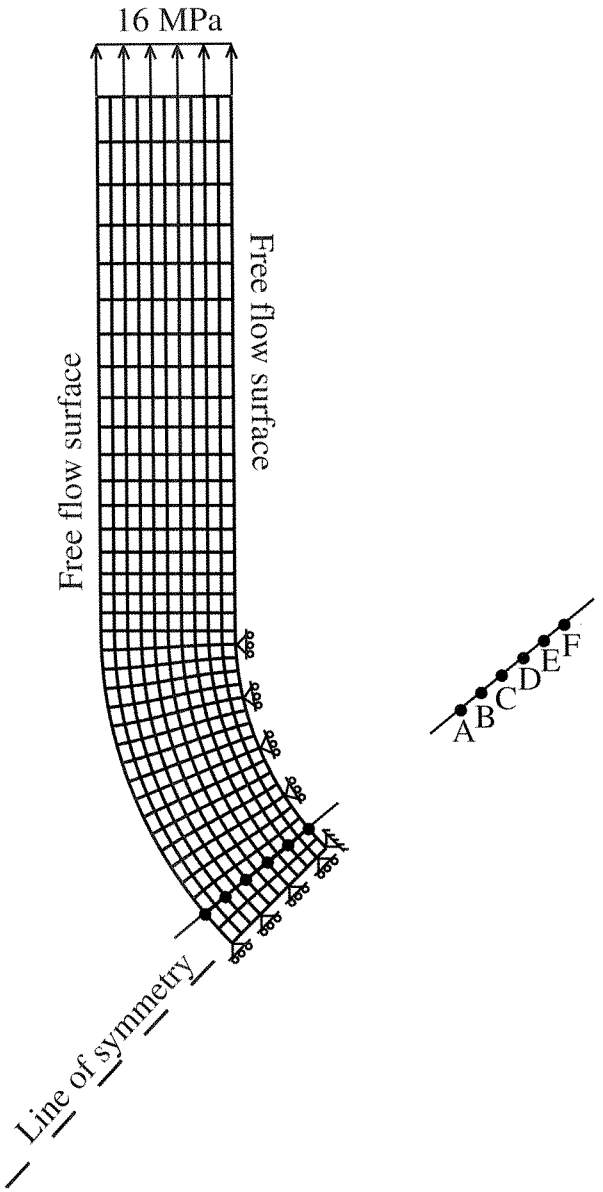

Figure 1.
Finite element model for rabbit flexor digitorum profundus tendon wrapping around talus.

Because a deep bony channel constrains the tendon's lateral (out-of-plane) motion, a two-dimensional plane strain formulation was used. The tendon, 1-mm wide and approximately 11-mm long, wrapped around a bone assumed to be circular with a 4-mm radius. Symmetry allowed modeling of only half of the tendon and was enforced by not allowing displacements across the line of symmetry. Disallowing radial displacement of the nodes abutting the bone enforced the constraint imposed by the bone. A uniform tensile traction of 16 MPa represented the loading applied at the proximal end of the tendon by its associated muscle.

The model used in this study differed from that of Giori and colleagues (17) in using four-noded hybrid elements with pore pressures (ABAQUS element CPE4PH) instead of standard four-noded hybrid plane strain elements (ABAQUS element CPE4H). The pore pressure elements implement the poroelastic constitutive model, with the ABAQUS implementation giving essentially the same results as custom codes for biphasic tissue behavior (24,25). Poroelastic and biphasic models are equivalent when the fluid phase is inviscid, as is usually assumed (23,24). Fluid was allowed to flow freely through the anterior and posterior surfaces of the tendon except in the region of bony contact (see **Figure 1**). Our analyses and those of Giori et al. (17) accounted for finite deformations and used hybrid elements to allow the solution of problems involving nearly incompressible materials.

As in the study of Giori et al. (17), reinforcing fibers representing type I collagen were included using the REBAR option in ABAQUS. The fibers were aligned parallel to the local longitudinal axis of the tendon and assigned an elastic modulus of 800 MPa to match the longitudinal elastic modulus of the tendon (26). The fibers were assumed to be nearly incompressible, with a Poisson's ratio of 0.497. The extrafibrillar matrix had a much lower modulus of 8 MPa and a Poisson's ratio of 0.1. These properties approximate those for other poroelastic or biphasic soft tissues, such as articular cartilage (24). The tissue was assigned an initial homogeneous water volume fraction of 67 percent, a value midway between the water volume fractions for the tendinous and fibrocartilaginous regions (3). Like Giori et al. (17), we assumed that the cells experience the same hydrostatic pressures as the extrafibrillar matrix.

Our first analysis demonstrates the general behavior of the poroelastic model using a homogeneous tendon with a relatively high permeability, $k=2\times10^{-1}$ m^4/Ns, to represent normal tendinous tissue (27). We examined the

time-dependent transfer of stresses between the fluid and solid constituents of the extrafibrillar matrix. We then investigated the effects of changing the permeability by repeating the first analysis with a lower permeability of 2×10^{-16} m^4/Ns to represent fibrocartilaginous tissue (28,29) and compared the results of the low-permeability analysis with those from the high-permeability case.

Finally, we studied adaptation of the tendon using cyclic hydrostatic pressure as the adaptation stimulus. We characterized the loading history with a hydrostatic pressure stimulus

$$\phi = [\Sigma_{day} n_i p_i^m]^{1/m}\Big|_{per\ day}, \quad [1]$$

where n_i is the number of cycles of load type i, p_i is either the maximum total hydrostatic pressure or the maximum hydrostatic fluid pressure for load type i, and m is an empirical constant. For convenience in this study, we simplified this expression by assuming a single load case and by assuming that the pressure magnitude affects the stimulus much more than the number of loading cycles, i.e., m is large. The stimulus then reduces to

$$\phi \approx p\Big|_{per\ day}, \quad [2]$$

Based on this stimulus, the permeabilities adapt to steady state values according to the relationship shown in **Figure 2**.

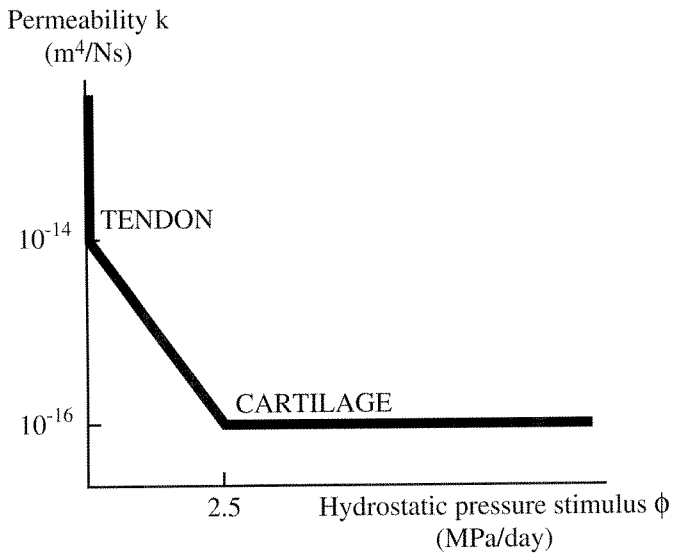

Figure 2.
Adaptation rule. Tissue permeability decreases with increased intermittent compressive hydrostatic stress. Fluid pressures and total hydrostatic pressures result in the same hydrostatic pressure stimulus.

Stimulus values near zero lead to permeabilities over 10^{-14} m^4/Ns as found in fibrous tissues such as tendon. Stimulus values above 2.5 MPa/day corresponding with intermittent hydrostatic pressures above 2.5 MPa lead to a low permeability of 10^{-16} m^4/Ns, representing cartilage. Intermediate stimulus values lead to intermediate permeabilities. The minimum pressure needed to maintain cartilaginous tissue is not known, but 2.5 MPa represents the lower end of physiologic cartilage pressures measured in the hip joint *in vivo* during normal activities of daily living (30,31).

The adaptation simulation started with a homogeneous tendon of permeability 10^{-14} m^4/Ns. Based on the hydrostatic pressure stimulus, the permeabilities changed according to the adaptation rule in **Figure 2**. For this simulation, we examined the predicted changes in tissue permeability as well as the fluid pressures and compressive stresses and strains in the solid matrix 1 s after load application. The 1-s time point represents a typical loading duration for physiologic activities such as slow walking.

RESULTS

The results of the first analysis illustrate the time-dependent transfer of stresses from the fluid to the solid constituents of the extrafibrillar matrix (**Figures 3** and **4**). Immediately after load application, the stresses are carried entirely by pressure in the fluid. The highest pressures appear where the tendon contacts the bone, and the pressures decrease with distance from the contact surface (**Figure 3, (a)**; t=0.001 s). Far from the contact surface, the pressure is approximately zero except near the line of load application, where modeling artifacts appear due to the simplified manner in which loading is applied to the upper end of the tendon. This profile of hydrostatic pressure closely resembles the hydrostatic stress profiles and magnitudes obtained using a single-phase elastic model (17).

While the fluid initially carries all of the stresses through pressurization, the fluid pressures dissipate over time as fluid flows out of the tissue. As the fluid pressures decrease, stresses transfer to the solid constituents of the extrafibrillar matrix (**Figure 3** and **Figure 4, (a), (b)**). At intermediate times such as t=1 s and t=5 s, stresses are shared between the fluid and solid, with the solid bearing higher stresses at later times (**Figure 3**). Eventually, all excess fluid pressures dissipate, leaving the solid phase to carry all the stresses (**Figure 4, (a), (b)**). An increase in

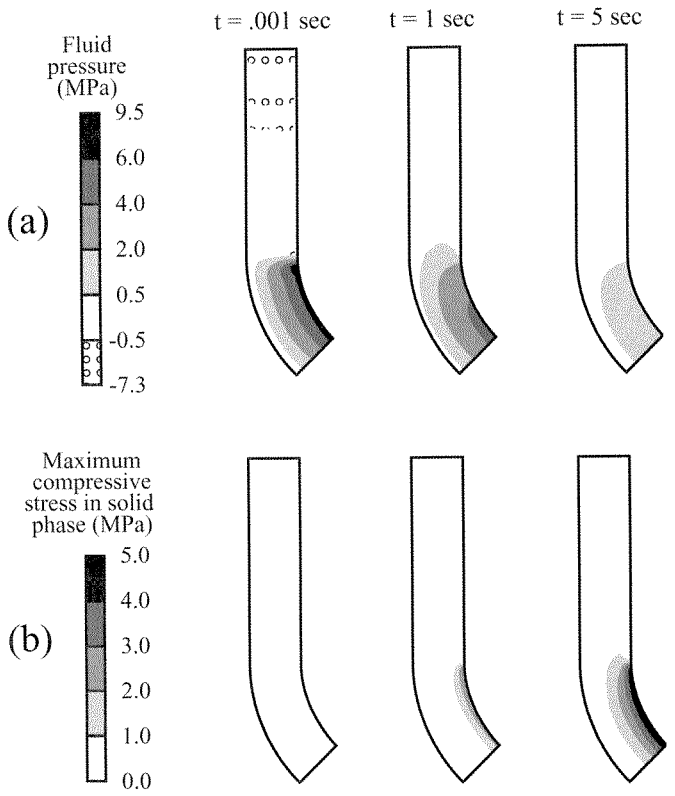

Figure 3.
Transfer of stresses from fluid to solid phase for the high-permeability case.

strains mirrors the increase in stresses in the solid phase over time (**Figure 4, (c)**).

When the tissue permeability decreases, the stresses still transfer from the fluid to the solid, but the transfer takes much longer because the low permeability restricts fluid flow (**Figure 5**). In the high-permeability case, all the fluid pressures dissipate in approximately 20 s. In the low-permeability case, the dissipation of fluid pressures takes approximately 2,000 s. The slower stress transfer means the solid phase is protected from high compressive stresses and strains for much longer periods of time. The results of the adaptation simulation (**Figure 6**) reflect these permeability effects. Prior to adaptation, the solid constituents sustain compressive strains up to 30 percent 1 s after load application. The adaptation produces a low-permeability region adjacent to the bone surface in an area corresponding to the fibrocartilaginous region. The low permeability allows the tissue in this region to maintain fluid pressures, reducing the compressive strains imposed on the solid constituents to less than 10 percent.

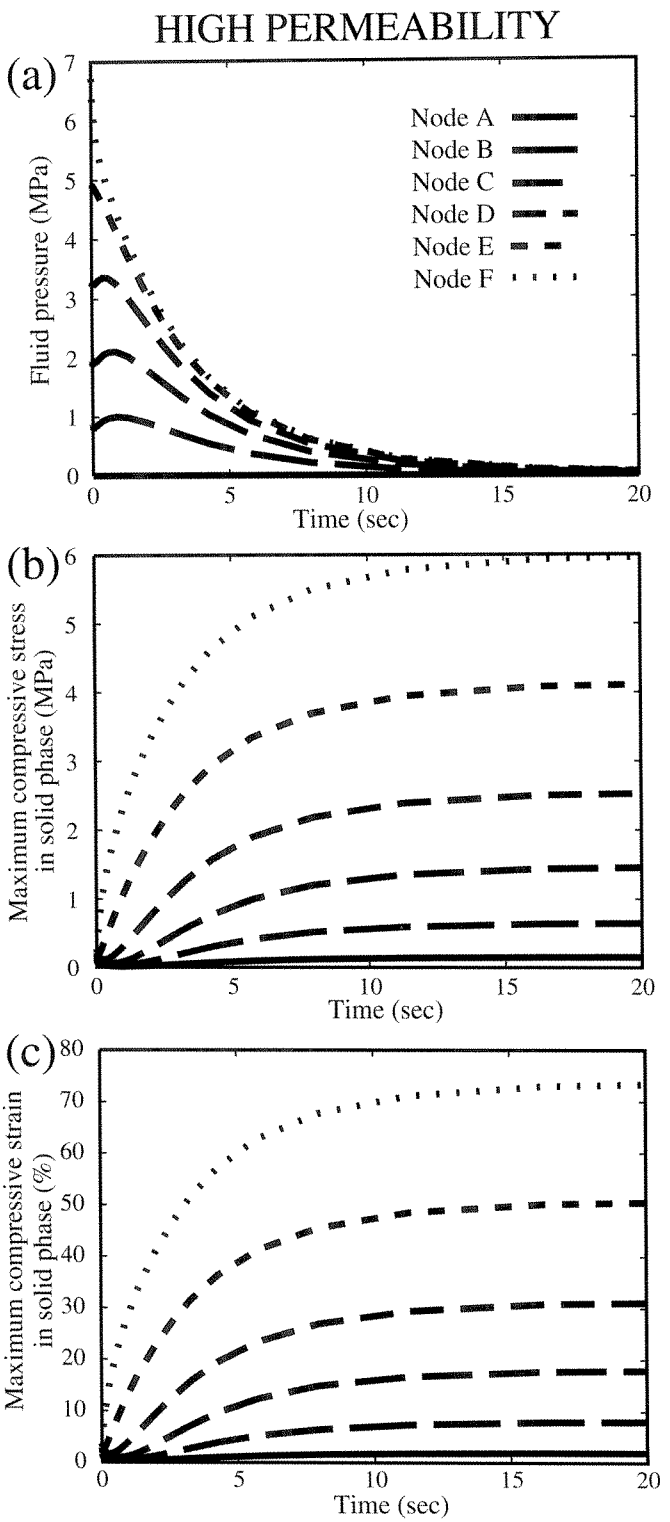

Figure 4.
Time-dependent changes in (a) fluid pressure, (b) maximum compressive stress in the solid phase, and (c) maximum compressive strain in the solid phase for the high-permeability case. Locations of nodes A–F are shown in **Figure 1.**

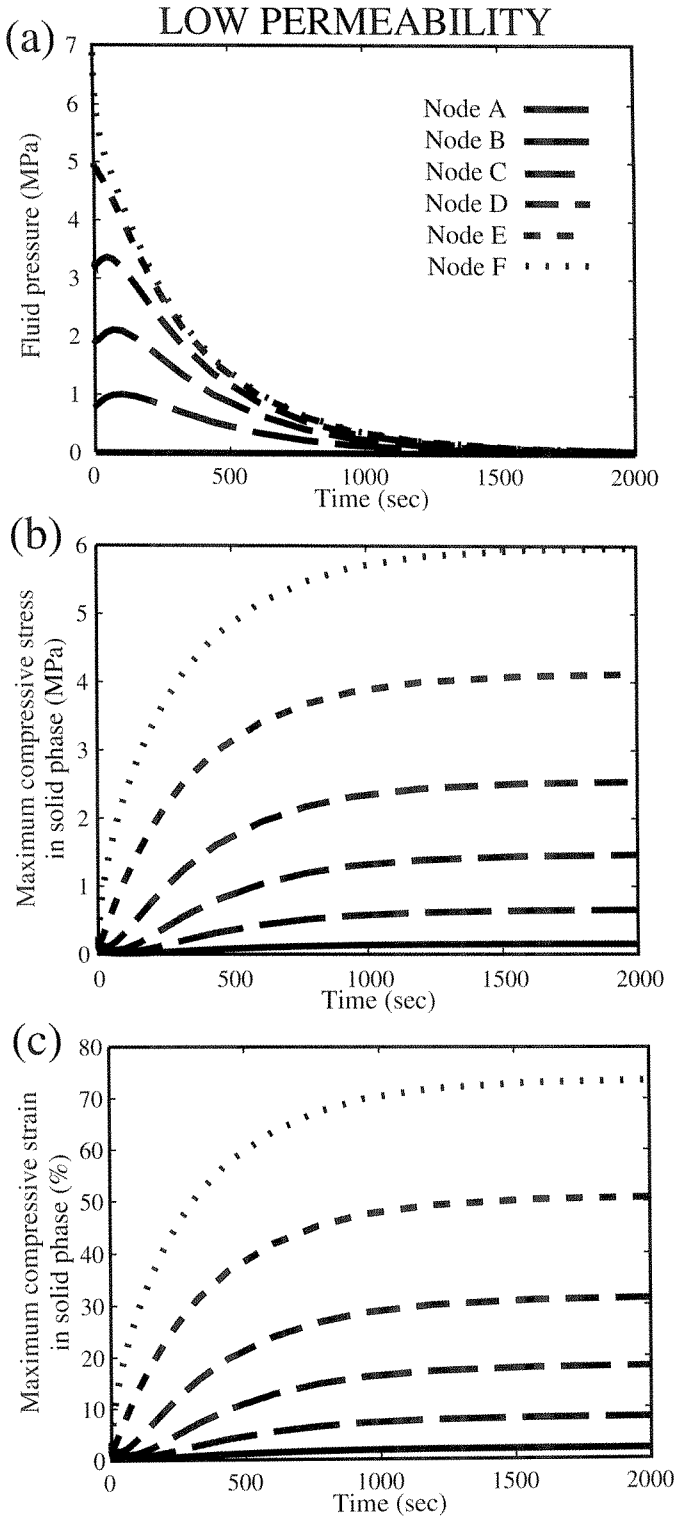

Figure 5.
Time-dependent changes in (a) fluid pressure, (b) maximum compressive stress in the solid phase, and (c) maximum compressive strain in the solid phase for the low-permeability case. Locations of nodes A–F are shown in **Figure 1.**

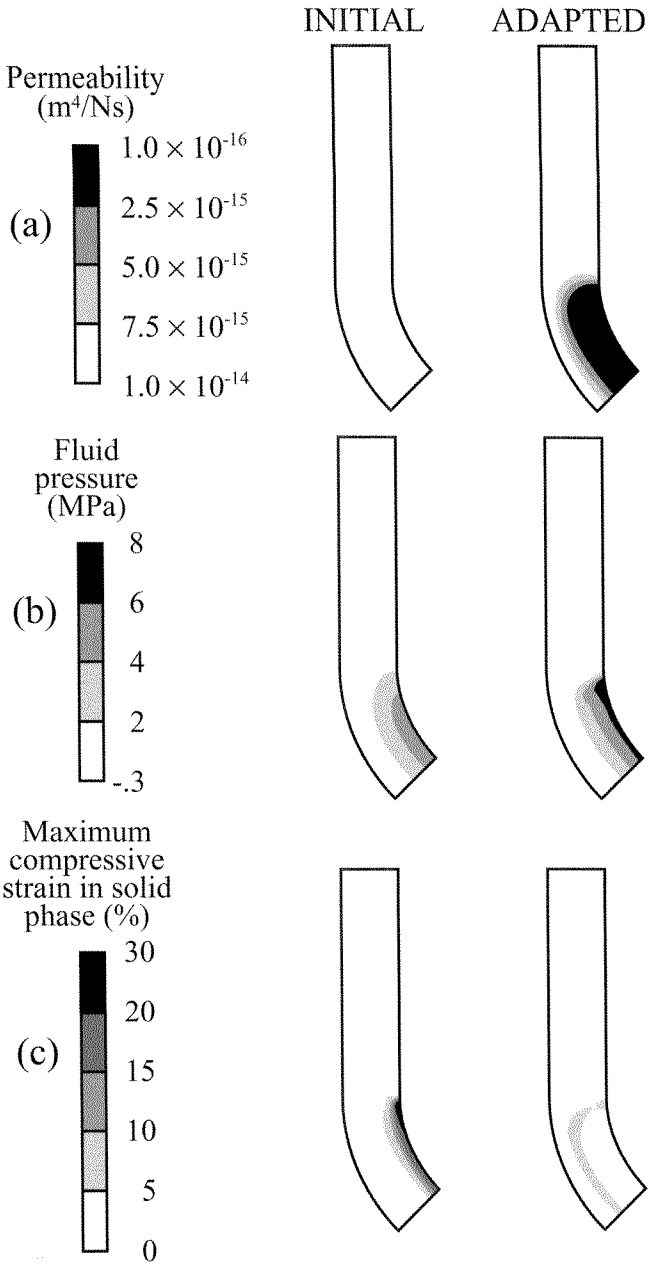

Figure 6.
(a) Permeabilities, (b) fluid pressures, and (c) maximum compressive strains in the solid phase, 1 s after load application during the adaptation simulation.

DISCUSSION

Many investigators have suggested that fibrocartilage develops in tendons in response to localized compressive loading (1,3,17,32). Robbins et al. (33) studied the effects of compressive loading on tendon segments *in vitro*. They found that both cyclic compressive loading

and TGF-β treatment up-regulated synthesis of aggrecan and biglycan, two important proteoglycans in cartilaginous tissue. Both treatments increased the expression of mRNA for TGF-β by 40 percent compared with unloaded samples, and the amount of newly synthesized TGF-β immunoprecipitated from extracts of loaded tissue was several times greater than that from unloaded tissue. Based on these findings, Robbins et al. (33) hypothesized that cyclic compressive loading increases TGF-β synthesis which then stimulates the synthesis of aggrecan and biglycan. This sequence may represent a pathway by which compressive loading leads to fibrocartilaginous metaplasia in tendons.

Although it appears clear that fibrocartilage formation in tendons is related to compressive loading, the stress states associated with the compressive loading are often poorly characterized. Giori and colleagues (17) were able to show that the location of fibrocartilage in the rabbit flexor digitorum profundus tendon corresponds with the specific stress state of hydrostatic compression or hydrostatic pressure (compressive stresses of equal magnitude from all directions). Building on those findings, we have proposed an adaptation rule based on a hydrostatic pressure stimulus. This adaptation rule predicts the development of a low-permeability region in the rabbit flexor digitorum profundus tendon corresponding to the fibrocartilaginous region observed *in vivo*.

In defining the hydrostatic pressure stimulus, we proposed that the stimulus take into account either peak fluid pressures or peak total hydrostatic pressures (sum of fluid pressures and compressive hydrostatic stresses in the solid phase). Peak fluid pressures occur when the loading is first applied. Peak total pressures occur at the same time and are equal to the peak fluid pressures. The same stimulus values are therefore obtained using either fluid pressures or total pressures in the adaptation stimulus. In addition, because the peak fluid pressures from the poroelastic model are essentially the same as the hydrostatic pressures from an elastic model (17), similar stimulus values could be obtained using hydrostatic pressures from a single-phase elastic model. Currently, the transduction mechanisms for hydrostatic pressures are not known. Hydrostatic pressures may be transmitted to the cells through only the fluid phase of the extracellular matrix or through both the fluid and solid phases.

Although we do not yet understand the mechanisms by which cells sense and respond to stresses including hydrostatic pressure, *in vitro* studies do suggest that hydrostatic pressures are a possible stimulus for the production of cartilaginous matrix constituents. Cultured chondrocytes increase their glycosaminoglycan synthesis when exposed to static or dynamic hydrostatic pressures up to 10 MPa (12,34). Cartilage explants also exhibit increased glycosaminoglycan synthesis when exposed to static or dynamic hydrostatic pressures up to 15 MPa (10,11,34).

The response of chondrocytes and cartilage explants to hydrostatic compression may differ from their response to other types of compressive loading associated with less well defined stress states. For example, uniaxial compression elicits different responses from cartilage explants depending on the magnitude and frequency of the applied loading. Static uniaxial compression inhibits glycosaminoglycan synthesis (35–37); dynamic uniaxial compression at fast rates stimulates glycosaminoglycan synthesis (36–38); and dynamic uniaxial compression at slow rates inhibits (36) or does not affect (37,38) glycosaminoglycan synthesis. For uniaxial compression, loading at fast rates creates high hydrostatic pressures, while static loading and dynamic loading at slow rates lead to fluid flow and tissue deformation instead of high hydrostatic pressures. With hydrostatic pressure as a mechanical stimulus, rapid dynamic uniaxial compression should stimulate, and static uniaxial compression should inhibit, glycosaminoglycan synthesis as observed experimentally.

Normal daily activities such as walking involve dynamic loading at rates on the order of 1 Hz. As we have shown in this study, such loading leads primarily to fluid pressurization with little fluid flow. Other theoretical analyses have also found that little fluid flow occurs in articular and epiphyseal cartilage during the short time periods associated with physiologic loading (37,39–41). In addition, experimental tests have shown that little fluid flow occurs when articular cartilage is subjected to oscillating compressive loads applied at physiologic frequencies (42). Consequently, for physiologic rates of loading, the material behavior of cartilaginous tissues such as tendon fibrocartilage can be well approximated as linear elastic and incompressible.

The utility of the poroelastic model lies in its ability to track the time-dependent transfer of stresses between the fluid and solid constituents of the extracellular matrix. Fibrocartilaginous metaplasia in tendons leads to compositional changes, including an increased content of proteoglycans such as aggrecan, and these changes reduce permeability in the fibrocartilaginous region. This decreased permeability slows the dissipation of fluid

pressures, shielding the solid matrix from high compressive stresses and strains during loading at physiologic rates. The tendon is thus protected from stresses and strains that could disrupt or damage its extracellular matrix organization.

The insights presented in this study were obtained using a relatively simple model to which many enhancements could be added. For example, viscoelastic collagen fiber behavior could be included, and tissue properties such as collagen fiber modulus and water content could be allowed to vary along with tissue permeability. Instead of the simplified hydrostatic pressure stimulus that we modeled, a more complex loading history—taking into account the hydrostatic pressure magnitude and number of cycles associated with multiple-load cases—could be examined. True dynamic loading could also be analyzed instead of the response to a single static load case over a 1-s interval. Even without these added complexities, however, we believe our model provides important and valid insights into the relationships between mechanics and fibrocartilaginous metaplasia in tendons.

The relationship between hydrostatic pressure and tissue differentiation and modulation along a cartilaginous pathway may apply not only to fibrocartilaginous metaplasia within tendons but to skeletal soft tissues more generally. Previous theoretical studies have correlated hydrostatic pressure with the appearance of cartilage in fracture calluses, pseudoarthroses, and fibrocartilaginous ligament insertions (14,15,43–45). The formation of fibrocartilage and cartilage may play a critical role in both successful fracture healing and failed fracture healing due to pseudoarthrosis formation. The development of fibrocartilage in the insertional regions of tendons and ligaments may also contribute to injuries affecting tendon and ligament insertions. The approaches introduced in this paper could be used to gain insight in these additional areas, and the mechanobiological principles presented herein may therefore have broad application in relating mechanics to soft tissue adaptation and injury.

CONCLUSION

Cyclic compressive hydrostatic stresses are a possible mechanical stimulus for fibrocartilaginous metaplasia in tendons. Cyclic hydrostatic pressures may stimulate changes in tendon cells toward a more chondrocytic phenotype, leading to increased synthesis of cartilaginous extracellular matrix components, including proteoglycans such as aggrecan. The resulting compositional changes lower the permeability of tissue in the fibrocartilaginous region. Decreased permeability allows the tissue to maintain fluid pressures for longer periods of time, reducing the compressive stresses and strains imposed on the solid constituents of the extracellular matrix. Thus, tendons adapt to cyclic compressive hydrostatic stresses through fibrocartilaginous metaplasia, protecting tendons from high compressive stresses and strains that could disrupt their extracellular matrix organization. This adaptation enables tendons to function effectively for an entire lifetime without sustaining excessive mechanical damage due to cyclic compressive loading.

ACKNOWLEDGMENTS

We would like to thank Vineet Sarin, Dr. R. Lane Smith, and Dr. Sheri D. Sheppard for their helpful suggestions.

REFERENCES

1. Benjamin M, Ralphs JR. Fibrocartilage in tendons and ligaments—an adaptation to compressive load. J Anat 1998;193:481–94.
2. Benjamin M, Qin S, Ralphs JR. Fibrocartilage associated with human tendons and their pulleys. J Anat 1995;187:625–33.
3. Okuda Y, Gorski JP, An K-N, Amadio PC. Biochemical, histological, and biomechanical analyses of canine tendons. J Orthop Res 1987;5:60–8.
4. Koob TJ, Vogel KG. Site-related variations in glycosaminoglycan content and swelling properties of bovine flexor tendon. J Orthop Res 1987;5:414–24.
5. Vogel KG, Ördög A, Pogány G, Oláh J. Proteoglycans in the compressed region of human tibialis posterior tendon and ligaments. J Orthop Res 1993;11:68–77.
6. Robbins JR, Vogel KG. Regional expression of mRNA for proteoglycans and collagen in tendon. Eur J Cell Biol 1994;64:264–70.
7. Sutker BD, Letster GE, Banes AJ, Dahners LE. Cyclic strain stimulates DNA and collagen synthesis in fibroblasts cultured from rat medial collateral ligaments. Trans Orthop Res Soc 1990;15:130.
8. Aggeler J, Frisch SM, Werb Z. Changes in cell shape correlate with collagenase gene expression in rabbit synovial fibroblasts. J Cell Biol 1984;98:1662–7.
9. Dhawan J, Farmer SR. Regulation of alpha 1 (I)-collagen gene expression in response to cell adhesion in Swiss 3T3 fibroblasts. J Biol Chem 1990;26:9015–21.
10. Hall AC, Urban JPG, Gehl KA. The effects of hydrostatic pressure on matrix synthesis in articular cartilage. J Orthop Res 1991;9:1–10.
11. Lippiello L, Kaye C, Neumata T, Mankin HJ. *In vitro* metabolic response of articular cartilage segments to low levels of hydrostatic pressure. Connect Tissue Res 1985;13:99–107.

12. Smith RL, Rusk SF, Ellison BE, Wessells P, Tsuchiya K, Carter DR, et al. *In vitro* stimulation of articular chondrocyte mRNA and extracellular matrix synthesis by hydrostatic pressure. J Orthop Res 1996;14:53–60.
13. Toyoda T, Saito S, Inokuchi S, Yabe Y. The effects of tensile load on the metabolism of cultured chondrocytes. Clin Orthop 1999;359:221–8.
14. Pauwels F. A new theory concerning the influence of mechanical stimuli on the differentiation of the supporting tissues. In: Biomechanics of the locomotor apparatus. Berlin: Springer-Verlag; 1980. p. 375–407.
15. Carter DR, Blenman PR, Beaupré GS. Correlations between mechanical stress history and tissue differentiation in initial fracture healing. J Orthop Res 1988;6:736–48.
16. Carter DR, Giori NJ. Effect of mechanical stress on tissue differentiation in the bony implant bed. In: Davies JE, editor. The bone-biomaterial interface. Toronto: University of Toronto Press; 1991. p. 376–9.
17. Giori NJ, Beaupré GS, Carter DR. Cellular shape and pressure may mediate mechanical control of tissue composition in tendons. J Orthop Res 1993;11:581–91.
18. Mow VC, Holmes MH, Lai WM. Fluid transport and mechanical properties of articular cartilage: A review. J Biomech 1984;17:377–94.
19. Hardias B, Butler DL, Malaviya P, Awad HA, Boivin GP, Smith FNL, et al. *In vivo* stresses correlate with cellular morphology in the fibrocartilage-rich region of the rabbit flexor tendon. Trans Orthop Res Soc 1998;23:21.
20. Favenesi JA, Shaffer JC, Mow VC. Biphasic mechanical properties of knee meniscus. Trans Orthop Res Soc 1983;8:57.
21. Frank EH, Grodzinsky AJ. Cartilage electromechanics—II. A continuum model of cartilage electrokinetics and correlation with experiments. J Biomech 1987;20:629–39.
22. Mow VC, Hou JS, Owens JM, Ratcliffe A. Biphasic and quasilinear viscoelastic theories for hydrated soft tissues. In: Mow VC, Ratcliffe A, Woo SL-Y, editors. Biomechanics of diarthrodial joints, volume I. New York: Springer-Verlag; 1990. p. 215–60.
23. Simon BR. Multiphasic poroelastic finite element models for soft tissue structures. Appl Mech Rev 1992;45:191–218.
24. Wu JZ, Herzog W, Epstein M. Evaluation of the finite element software ABAQUS for biomechanical modeling of biphasic tissues. J Biomech 1998;31:165–9.
25. van der Voet AF. Discussion. A comparison of finite element codes for the solution of biphasic poroelastic problems. J Eng Med, Proc Part H 1996;210:209–11.
26. Gibbons DF. Biomedical materials. In: Fleming DG, Feinberg BN, editors. Handbook of engineering in medicine and biology. Cleveland: CRC Press; 1976. p. 254.
27. Chen C-T, Malkus DS, Vanderby R Jr. A fiber matrix model for interstitial fluid flow and permeability in ligaments and tendons. Biorheology 1998;35:103–18.
28. Maroudas A. Physiochemical properties of articular cartilage. In: Freeman MAR, editor. Adult articular cartilage. 2nd ed. Kent: Pitman Medical Publishing Co. Ltd.; 1989. p. 215–90.
29. Mansour JM, Mow VC. The permeability of articular cartilage under compressive strain and at high pressures. J Bone Joint Surg Am 1976;58(4):509–16.
30. Hodge WA, Carlson KL, Fijan RS, Burgess RG, Riley PO, Harris WH, et al. Contact pressures from an instrumented hip endoprosthesis. J Bone Joint Surg Am 1989;71(9):1378–86.
31. Hodge WA, Fijan RS, Carlson KL, Burgess RG, Harris WH, Mann RW. Contact pressures in the human hip joint measured *in vivo*. Proc Natl Acad Sci U S A 1986;83:2879–83.
32. Gillard GC, Reilly HC, Bell-Booth PG, Flint MH. The influence of mechanical forces on the glycosaminoglycan content of the rabbit flexor digitorum profundus tendon. Connect Tissue Res 1979;7:37–46.
33. Robbins JR, Evanko SP, Vogel KG. Mechanical loading and TGF-beta regulate proteoglycan synthesis in tendon. Arch Biochem Biophys 1997;342:203–11.
34. van Kampen GPJ, Veldhuijzen JP, Kuijer R, van de Stadt RJ, Schipper CA. Cartilage response to mechanical force in high-density chondrocyte cultures. Arthritis Rheum 1985;28:419–24.
35. Jones IL, Klämfeldt A, Sandström T. The effect of continuous mechanical pressure upon the turnover of articular cartilage proteoglycans *in vitro*. Clin Orthop 1982;165:283–9.
36. Palmoski MJ, Brandt KD. Effects of static and cyclic compressive loading on articular cartilage plugs *in vitro*. Arthritis Rheum 1984;27:675–81.
37. Sah RL-Y, Kim Y-J, Doong J-YH, Grodzinsky AJ, Plaas AHK, Sandy JD. Biosynthetic response of cartilage explants to dynamic compression. J Orthop Res 1989;7:619–36.
38. Parkkinen JJ, Lammi MJ, Helminen JH, Tammi M. Local stimulation of proteoglycan synthesis in articular cartilage explants by dynamic compression *in vitro*. J Orthop Res 1992;10:610–20.
39. Armstrong CG, Lai WM, Mow VC. An analysis of the unconfined compression of articular cartilage. J Biomech Eng 1984;106:165–73.
40. Brown TD, Singerman RJ. Experimental determination of the linear biphasic constitutive coefficients of human fetal proximal femoral chondroepiphysis. J Biomech 1986;19:597–605.
41. Ateshian GA, Lai WM, Zhu WB, Mow VC. An asymptotic solution for the contact of two biphasic cartilage layers. J Biomech 1994;27:1347–60.
42. Higginson GR, Snaith JE. The mechanical stiffness of articular cartilage in confined oscillating compression. Eng in Med 1979;8:11–4.
43. Matyas JR, Anton MG, Shrive NG, Frank CB. Stress governs tissue phenotype at the femoral insertion of the rabbit MCL. J Biomech 1995;28:147–57.
44. Carter DR, Beaupré GS, Giori NJ, Helms JA. Mechanobiology of skeletal regeneration. Clin Orthop 1998;355(Suppl):S41–55.
45. Carter DR, van der Meulen MCH, Beaupré GS. Mechanobiologic regulation of osteogenesis and arthrogenesis. In: Buckwalter JA, Ehrlich MG, Sandell LJ, Trippel SB, editors. Skeletal growth and development: Clinical issues and basic science advances. Rosemont: American Academy of Orthopaedic Surgeons; 1998. p. 99–130.